Rapidly Responsive Smart Adhesive-Coated Micropillars Utilizing Catechol-Boronate Complexation Chemistry

Ameya R. Narkar[1], **Chito Kendrick**[2], **Kishan Bellur**[3], **Timothy Leftwich**[4], **Zhongtian Zhang**[1], **Bruce P. Lee**[1]

[1]Department of Biomedical Engineering, Michigan Technological University, Houghton, MI 49931

[2]Department of Electrical and Computer Engineering, Michigan Technological University, Houghton, MI 49931

[3]Department of Mechanical Engineering-Engineering Mechanics, Michigan Technological University, Houghton, MI 49931

[4]Department of Materials Science and Engineering, Michigan Technological University, Houghton, MI 49931

Abstract

Smart adhesive hydrogels containing 10 mol % each of dopamine methacrylamide (DMA) and 3-acrylamido phenylboronic acid (APBA) were polymerized in situ onto polydimethylsiloxane (PMDS) micropillars with different aspect ratio (AR = 0.4, 1 and 2). Using Johnson-Kendall-Roberts (JKR) contact mechanics tests, the adhesive-coated pillars demonstrated strong wet adhesion at pH 3 ($W_{adh} = 420$ mJ/m^2) and can be repeatedly deactivated and reactivated with changing pH (pH 9 and 3, respectively). When compared to bulk adhesive hydrogel of the same composition, adhesive-coated pillar exhibited significantly faster rate of transition (1 min) between strong and weak adhesion. This was attributed to an increased surface area to volume ratio of the adhesive hydrogel-coated pillars, which permitted rapid diffusion of ions into the adhesive matrix to form or break the catechol-boronate complex.

Introduction

Smart adhesives that can rapidly transition between strong and weak adhesion upon the application of external stimuli can be of great practical significance in various potential applications including painless removal of wound dressings, effortless disassembly of bonded structural components, sustainable recycling of materials without damaging substrates, and controlled locomotion of robots.[1–4] Current smart adhesives have limited applications due to slow responsiveness and the need for extreme conditions for bonding or debonding (e.g., high temperature,[3] harmful UV exposure[5]). Most importantly, many smart adhesives are unable to bind to wetted surfaces.[6] For biomedical and underwater applications, it is desirable for a smart adhesives to be able to rapidly and reversibly bind to surfaces in a wet environment.

Marine mussels secrete adhesive foot proteins that contain a unique catecholic amino acid, 3,4-dihydroxyphenylalanine (DOPA), which is responsible for adhesion to wetted surfaces

(e.g. rocks, piers, etc.).[7, 8] Catechol functionalization of inert polymers has been used to design adhesives for various applications.[9–11] Additionally, smart adhesives containing catechol that respond to externally applied stimuli such as light,[12] enzyme[13] or temperature[14] have been previously reported. Recently, our lab reported a pH-responsive smart adhesive based on the reversible complexation chemistry between catechol and boronic acid.[15, 16] At an acidic pH, catechol and boronic acid contributed to adhesion, while at a at basic pH, the complexation between catechol and boronic acid led to reduced adhesion. The adhesion at an acidic pH was an order of magnitude higher than at a basic pH, and the adhesive demonstrated reversible switching between strong and weak adhesion in response to changing pH. The network bound boronic acid acted as a protecting group to prevent catechol oxidation and to preserved reversibility of catechol for interfacial binding. However, these hydrogel-based adhesives required an extensive period of incubation (30 min to 60 min) to be deactivated or reactivated for adhesion, potentially due to slow diffusion of ions into the adhesive network for the formation or dissociation of the catechol-boronate complex. Thus, there is still a need to increase the rate at which the adhesive could reversibly switch between its adhesive and non-adhesive states.

To increase the rate of switching, one possible solution is to coat the adhesive hydrogel onto a surface with an array of micron-scaled features. The increase in surface area due to the smaller features has been shown to offer strong dry adhesion owing to the contact-splitting phenomenon.[17] However, the adhesion of such micropillars was dramatically reduced in the presence of moisture.[18] Catechol containing-polymers have been previously coated onto pillars to enhance strong wet adhesion and multiple cycles of attachment and detachment.[19–21] However, these adhesive-coated pillars did not demonstrate tunable adhesive property. In this paper, smart adhesive based on catechol-boronate chemistry were coated on microfabricated pillars, thereby increasing the surface area to volume ratio of the adhesives. We hypothesize that the increased surface area to volume ratio could potentially lead to an increase in rate of diffusion of ions necessary to change pH within the adhesive network, thus causing faster formation and breaking of the complexation.

Here, polydimethyl siloxane (PDMS) micropillars with three different aspect ratios were coated with an adhesive hydrogel containing dopamine methacrylamide (DMA) and 3-acrylamido phenylboronic acid (APBA). Dopamine contains a catechol functional group and mimics the interfacial binding chemistry of DOPA. The presence of the adhesive hydrogel coating was verified using Field emission-scanning electron microscopy (FE-SEM), while Fourier Transform Infrared Spectroscopy (FTIR) and X-ray Photoelectron Spectroscopy (XPS) were used for chemical characterization. The effect of micropatterning and adhesive hydrogel coating on the rapid reversible adhesion was examined using Johnson-Kendall Roberts (JKR) contact mechanics test.

Materials and Methods

Materials

APBA, *N*-hydroxyethyl acrylamide (HEAA) and 3-(trimethoxysilyl)propyl methacrylate (TMSPMA), trichloro(1H,1H,2H,2H-perfluorooctyl)silane were purchased from Sigma-Aldrich (St. Louis, MO). Methylene bis-acrylamide (MBAA) and 2,2-dimethoxy-2-

phenylacetophenone (DMPA) were purchased from Acros Organics (New Jersey, USA). Dimethyl sulfoxide (DMSO) was purchased from Macron (Center Valley, PA), and ethanol (200 proof) were purchased from Pharmco Aaper (Brookfield, CT). Hydrogen peroxide (30% stock solution) (H_2O_2) was purchased from Fisher Scientific (Fair Lawn, NJ). Polydimethylsiloxane (PDMS) monomer and crosslinking agent (Sylgard 184 Silicone Elastomer kit) were purchased from Dow Corning (Midland, MI). DMA was synthesized by following previously published protocols.[19] The acidic pH 3.0 solution was prepared by adding 1 M HCl to deionized (DI) water. The pH 9.0 buffer solution was prepared by adjusting the pH of 10 mM Tris (hydroxymethyl) aminomethane (Tris) buffer with 1 M HCl.

Methods

Preparation of PDMS with bare micropillars—Silicon (Si) master molds were created with arrays pores of depths of 4-20 μm, diameter (d) of 10 μm, and pitch (p) of 20 μm using protocols described in the Supporting Information. The Si master molds were cleaned with N_2 gas. A silane passivation layer was deposited onto the master mold to enable easy peel-off of PDMS. To do this, the master molds were placed inside a desiccator chamber in which two drops (≈ 100 μL) of the silanizing agent, trichloro(1H,1H,2H,2H-perfluorooctyl)silane were placed on a glass slide beside the master mold. The desiccator chamber was pumped down for 10 min using a vacuum pump to accelerate the evaporation of silane and maintained in a sealed condition for 10 additional minutes. The master mold was retrieved and placed on a hot plate at 150°C for 10 min to evaporate the excess silane. A mixture of PDMS prepolymer and curing agent (10:1 weight ratio) was degassed, poured over the Si master mold and cured at 60°C for 4 hours. The cured PDMS was allowed to cool overnight and then peeled off, and the surface of PDMS was further washed with ethanol and deionized (DI) water. PDMS micropillars with heights (h) of 4-20 μm, diameter (d) of 10 μm, and pitch (p) of 20 μm were fabricated. These micropillars of different aspect ratios (ARs) are denoted as 'Bare-ARx', where x represents the AR of the pillars (AR = h/d).

Coating the PDMS micropillars with adhesive hydrogel—Adhesive hydrogels were chemically linked to the PDMS micropillars by *in situ* photopolymerization (Schemes S1, S2 and S3). The surface of the micropillars was first functionalized with polymerizable methacrylate group, TMSPMA, following a previously published protocol.[22] Briefly, the surface of PDMS was treated with oxygen plasma at 100 W and 200 mTorr for 1 min (Jupiter II, March Instruments; Westlake, OH). The pillars were then immersed in a solution containing H_2O, H_2O_2, and HCl with a volume ratio of 5:1:1 for 5 min followed by a DI water rinse. The pillars were further introduced into a 1.5 v/v % TMSPMA solution in ethanol-DI water mixture (volume ratio of 1:1) for 1 hour. The samples were washed with DI water and dried with compressed air and N_2.

To prepare the adhesive hydrogel-coated micropillars, 6 μL of 0.1 mol % DMPA solution in ethanol was first added to TMSPMA-modified pillars. A precursor solution was prepared by dissolving 1 M of HEAA with 10 mol % each of DMA and APBA and 0.1 mol% of DMPA and 3 mol% of MBAA in 40% (v/v) DMSO in DI water and degassed three times with N_2 gas. 10 μL of the precursor solution was added to the micropillars, which was covered with a cover glass and photoinitiated for 100 sec in a UV cross-linking chamber (XL-1000,

Spectronics Corporation; Westbury, NY) located in a nitrogen-filled glovebox (PLAS LABORATORIES; Lansing, MI).[23, 24] The adhesive hydrogel-coated micropillars were washed in DI water for overnight with gentle nutation. For comparison purposes, flat adhesive films were prepared by photopolymerizing the precursor solution containing 0.1 mol % DMPA in a mold composed of two glass pieces separated by a silicone rubber spacer (0.75 mm thick) for a total of 200 sec.[25] The adhesive hydrogel-coated micropillars were denoted as 'AD-ARx' where 'x' represents the AR of the pillars and the flat adhesive film was denoted as 'AD-Flat'.

Characterization of the adhesive-coated micropillars—The morphology of the samples was characterized using field emission-scanning electron microscopy (FE-SEM; S-4700, Hitachi; Tarrytown, NY). Samples were incubated in pH 3 for 5 min and air-dried for at least 72 hours before imaging. For contact angle measurement, hydrated samples were maintained in a parafilm-sealed petri dish along with 200 μL of pH 3 buffer for 30 minutes before analysis. A drop of approximately 0.66 μL of DI water was manually placed on the sample surface using $1/8^{th}$ rotation of a threaded plunger syringe (81242, Hamilton; Reno, NV) fitted with a small gauge metal needle. The droplet image was taken 10 s after the deposition of the liquid. The contact angle measurement was performed at three separate locations on each sample using ImageJ software. (See Supporting Information for details regarding the imaging setup). For attenuated total reflection (ATR) Fourier-transform infrared (FTIR) spectroscopy analysis, samples were dried with vacuum for overnight, pressed against a diamond crystal window with a constant number of turns, and analyzed using a PerkinElmer Spectrum One Spectrometer (Waltham, MA) fitted with a GladiATR accessory from Pike Technologies (Madison, WI). For X-ray photoelectron spectroscopy analysis, vacuum-dried samples were analyzed using a PHI 5800 X-ray photoelectron spectrometer (Physical Electronics; Chanhassen, MN). The results were further analyzed using Origin. Detailed protocol for XPS analysis is available in Supporting Information.

JKR Contact Mechanics Test—JKR contact mechanics test was performed to determine the interfacial binding properties of the adhesive hydrogel-coated micropillars. A custom-built indentation device equipped with a 10-g load cell (Transducer Techniques; Temecula, CA) and a high resolution miniature linear step motor (MFA-PPD, Newport; Irvine, CA)[15, 16] was used in conjunction with a SiO_2 hemisphere with a diameter of 6 mm and a thickness of 3 mm (QU-HS-6, ISP Optics; Irvington, NY) as the contacting surface. During a typical contact cycle, the SiO_2 hemisphere was compressed against the sample at 0.5 μm/sec until a maximum preload (10-80 mN) was reached. The surface maintained contact with the substrate for 30 sec and was then retracted at the same rate.

Two separate contact mechanics experiments were performed. In the first experiment, the effect of pH on the interfacial binding property was evaluated. Samples were incubated with either pH 3 or 9 buffer solution for 5 min. Then a single contact cycle was carried out in the presence of 2 μL of the same buffer solution. In the second experiment, the ability for a single sample to repeatedly transition between its adhesive and non-adhesive states in response to changes in pH was determined. A given sample was subjected to successive contact cycles. The sample washed in DI water was incubated at pH 3 for 5 min prior to the

first contact cycle. The first and the subsequent odd numbered contacts were carried out in the presence of 2 μL of pH 3 solution, while the second and subsequent even numbered contacts were carried out in the presence of 2 μL of pH 9 solution. Between cycles, the samples were briefly rinsed in DI water and incubated for 1-5 min in a petri dish containing 10 mL of either pH 9 (between odd numbered and even numbered cycle) or pH 3 (between even numbered and odd numbered cycles) solutions.

The force (F) versus displacement (δ) curves were integrated to determine the work of adhesion (W_{adh}), which was normalized by the apparent maximum area of contact (A_{max}) while assuming the contact area of a flat surface.[26] W_{adh} was calculated by using the following equation:[15]

$$W_{adh} = \frac{\int F \, d\delta}{A_{max}}, \quad (1)$$

where A_{max} was calculated by fitting the loading portion of the F versus δ curve with the Hertzian model:[27]

$$\delta_{max} = \frac{a^2}{R}, \quad (2)$$

where δ_{max} is the maximum displacement at the applied maximum preloads (10-80 mN), a is the radius of A_{max}, and R is the curvature of the hemispherical SiO_2 indenter. The thickness (t = 3 mm) and base radius (r = 3 mm) of the SiO_2 hemisphere was used to determine R:[28]

$$R = \frac{t}{2} + \frac{r^2}{2t} \quad (3)$$

A_{max} was calculated by using the equation:

$$A_{max} = \pi a^2 \quad (4)$$

The adhesion strength (S_{adh}) was calculated by normalizing the maximum pull-off force (F_{max}) by the apparent maximum area of contact (A_{max}) using the equation:[29]

$$S_{adh} = \frac{F_{max}}{A_{max}} \quad (5)$$

The Young's modulus (E) was obtained by fitting the advancing portion of the F versus δ curve using the equation:[27]

$$F = \frac{16R^{1/2}E\delta^{3/2}}{9} \quad (6).$$

Statistical Analysis—Statistical analysis was performed using One-way analysis of variance (ANOVA) with Tukey-Kramer HSD analysis using JMP Pro 13 application (SAS Institute, NC). $p < 0.05$ was considered statistically significant.

Results and Discussion

Characterization of adhesive hydrogel-coated micropillars

Micropillars with AR between 0.4 and 2 were coated with adhesive hydrogels containing both DMA and APBA. To ensure that the hydrogels were covalently crosslinked to the micropillars, the surface of the micropillars were first grafted with polymerizable methacrylate group using silane chemistry followed by *in situ* photo-initiated polymerization (Scheme S1). FE-SEM images confirmed the presence of the hydrogel coating (Figure 1). The edges of the unmodified, bare micropillars initially appeared sharp with nano-scaled features along the vertical surfaces of the pillars, which was due to the BOSCH process used to create the Si master mold of the desired depths. These sharp edges and features disappeared after the micropillars were coated with the adhesive hydrogel and the surfaces of adhesive-coated micropillars appeared smooth. An equal volume of precursor solution was used for the micropillars with different ARs and the precursor solution ended up filling the interstitial spaces between the pillars, effectively shortening the adhesive-coated pillars. In case of AD-AR0.4 (Figure 1d), the micropillars were obscured by the coating and appeared like a bumpy surface. For AD-AR1, an appreciable height of the pillars was still visible after the coating (Figure 1e). When Bare-AR2 was coated with the adhesive, it settled toward the bottom of the pillars, and likely formed a web like pattern due to the relatively lower volume of precursor as compared to the volume of interstitial spaces (Figure 1f).

The wetting behavior of the bare and adhesive hydrogel-coated micropillars was evaluated by performing water contact angle measurements. The representative water contact angle images can be seen in Figure S1. Contact angle measured for flat PDMS was $110.0 \pm 2.7°$, which in agreement with published values.[30] Contact angle values of bare micropillars were 25-40° higher and these values increased with increasing AR (Table 1). This was due to the increased volume of air trapped between the pillars with increasing AR, which increased hydrophobicity.[31] The contact angle values for the adhesive-coated micropillars were lower than those for the bare micropillars. Coating the pillars with hydrophilic hydrogel effectively lowered the contact angle values by 20-30°, confirming the presence of the adhesive hydrogel coating. Water contact angle for Flat-AD ($69.8 \pm 3.6°$) was significantly lower when compared to that of flat PDMS. However, the contact angle for AD-AR2 was around 15° higher than those of AD-AR0.4 or AD-AR1. This may be potentially due to reduced coverage of the adhesive hydrogel on the pillars with the highest AR.

FTIR spectra further confirmed the presence of the hydrogel coating (Figure 2). The spectra for bare micropillars exhibited the typical features of PDMS associated with Si-CH$_3$

(2960-2950 cm^{-1}, 1260-1259 cm^{-1} and 796-789 cm^{-1}) and Si-O-Si (1074-1020 cm^{-1}).[32] The spectrum for the adhesive-coated micropillars exhibited additional features as found in AD-Flat, associated with HEAA (hydroxyl group at 3400-3000 cm^{-1}, secondary amide at 1680-1630 cm^{-1}, and C=O at 1600-1500 cm^{-1}) and benzene rings found in catechol and phenylboronic acid (1500-1400 and 800-700 cm^{-1}).[15] The spectra for DMA and APBA were also measured (Figure S2) and the functional groups are in agreement with previous reports.[20, 33, 34] For AD-AR2, there was a drastic reduction in the peak intensity associated with the adhesive hydrogel when compared to those corresponding to PDMS, indicating that there is a reduced coverage of the adhesive. Regardless of the micropillar AR, the same volume of precursor solution was used for coating. The reduced adhesive peak intensity is associated with the coating being present toward the bottom of the pillars due to a higher interstitial volume of the micropillars when compared to pillars with lower ARs.

The adhesive hydrogel-coated micropillars were further characterized using XPS (Figure 3). Bare micropillars exhibited peaks associated with oxygen (1s, 530.8 eV), carbon (1s, 284.8 eV) and silicon (2s, 153 eV and 2p, 103 eV) typically found for PDMS.[19, 35, 36] For adhesive-coated micropillars, additional peaks corresponding to nitrogen (1s, 399 eV) and boron (1s, 191.5 eV)[37] were found, which indicated the presence of the adhesive hydrogel.

Contact Mechanics Test

The effect of pH on the interfacial binding property of the adhesive hydrogel-coated micropillars was evaluated using JKR contact mechanics test (Figure 4). Bare micropillars with different ARs exhibited low adhesion values (W_{adh} < 75 mJ/m^2 and S_{adh} < 2.7 kPa) to SiO$_2$ surface. This is because the pillars rely on van der Waals forces for interacting with the substrate surface, which are significantly weakened in the presence of moisture.[18, 38] On the other hand, adhesive-coated micropillars with AR of 0.4 and 1 demonstrated strong adhesion to the SiO$_2$ surface when tested at pH 3 (W_{adh} = 300-420 mJ/m^2 and S_{adh} ~ 17 kPa), indicating that the presence of catechol is required for strong, moisture resistant interfacial binding. Both the catechol and boronic acid found in the adhesive hydrogel contributed to interfacial binding potentially through the formation of hydrogen bonds with SiO$_2$ (Scheme S3).[15] However, AD-AR2 exhibited poor adhesion. This is potentially due to inadequate coverage of the adhesive hydrogel due to a large interstitial space between pillars for AD-AR2 and the use of same volume of precursor solution for coating. FTIR spectrum of AD-AR2 confirmed lower peak intensity associated with the adhesive hydrogel when compared to micropillars with lower ARs (Figure 2). For micropillared structures tested in a dry environment, adhesion typically increases with increasing AR.[26] Our results here further confirmed that the catechol-containing adhesive coating is required for strong adhesion to wet surfaces. Flat adhesive film (AD-Flat) exhibited elevated W_{adh} value (262.3 ± 17.67 mJ/m^2) but a low S_{adh} value (1.952 ± 0.1242 mJ/m^2). The Young's modulus for the flat hydrogel is significantly lower than that of the PDMS micropillars, which resulted in significantly higher area of contact (A_{max}) and reduced S_{adh} value (Figure S3).

Although both AD-AR0.4 and AD-AR1 demonstrated strong adhesion at pH 3, their W_{adh} and S_{adh} values reduced significantly when tested at pH 9 (~ 4 and 14-fold reduction, respectively; Figure 4b and d). These adhesive values were not statistically different when

compared to those measured for the unmodified, bare micropillars (Table S1), indicating that changing pH effectively inactivated that adhesive property of the adhesive-coated pillars (Scheme S3). FTIR spectra of the adhesive-coated micropillars performed at pH 9 exhibited a new peak at 1495 cm^{-1} corresponding to the catechol-boronate complex (Figure S4).[39] This observation is in agreement with our previous published reports, which indicated that catechol-boronate complexation reduces catechol's availability for interfacial binding.[15, 16] The W_{adh} values for AD-Flat continued to remain high at pH 9 (Figure 4b, Table S2). Although the FTIR spectrum of AD-Flat also exhibited catechol-boronate complex at pH 9 (Figure S4), the elevated adhesion property indicated that the formation of the complex was incomplete potentially due to a short incubation period (5 min) in the basic buffer and the slow diffusion of ions into the bulk of the adhesive. Our previous work has shown that hydrogel-based adhesive required at least 30 min of incubation for complete inactivation.[15]

To determine the effect of preload on the adhesive behavior of the hydrogel-coated micropillars, the preload was varied from 10 to 80 mN. At any given preload, the W_{adh} values demonstrated by AD-AR1 were higher than those of AD-AR0.4 and AD-AR2 when tested at pH 3 (Figure 5a, Table S3). Additionally, W_{adh} values for AD-AR1 and AD-AR0.4 increased with increasing preload, potentially due to increased maximum area of contact (A_{max}) which increased proportionally with increasing preload (Figure S5, Table S7). However, the maximum pull-off (F_{max}) for AD-AR0.4 did not increase as rapidly (Table S7), which contributed to the decline in S_{adh} values with increased applied preload.

Increasing the surface area of the micropillars has been shown to enhance dry adhesion due to the contact-splitting phenomenon.[26] Our results for AD-AR1 indicated that both F_{max} and A_{max} increased with increasing preload, which potentially correlated to larger surface area of the adhesive-coated pillars that formed contact with the hemispherical probe. Additionally, S_{adh} for AD-AR1 remained constant with increasing preload (Figure 5c, Table S4). This is in agreement with previously published data which suggest that increasing the preload has a greater impact on adhesion in higher aspect ratio patterns.[26] Both the W_{adh} and S_{adh} values for the adhesive hydrogel-coated micropillars were significantly lower across the range of tested preloads at pH 9 (Figure 5b and d), as a result of catechol-boronate complexation. AD-AR2 showed low adhesion across the range of tested preloads regardless of pH.

Reversibility of adhesive-coated micropillars

To investigate the ability for the adhesive-coated micropillars to transition reversibly between its adhesive and non-adhesive state, samples were subjected to repeated contacts while changing pH between contact cycles. Both AD-AR0.4 and AD-AR1 exhibited changes in their adhesive property with changing pH (Figure 6 and Tables S12–15). Both adhesive formulations demonstrated elevated adhesive property during the first contact cycle tested at pH 3, which was reduced in the second contact cycle tested at pH 9. Particularly, the W_{adh} and S_{adh} values for AD-AR1 demonstrated a 74 and 94% reduction, respectively. Both adhesives recovered their original adhesive property when tested at pH 3 in the third contact cycle. FTIR results confirmed the formation (pH 9) and dissociation (pH 3) of the catechol-boronate complex in a pH dependent manner (Figure S6). These results indicated that catechol and boronic acid are reversibly bound, and can be used to tune the adhesive

property of the adhesive-coated micropillars. AD-AR2 showed negligible adhesion during the three successive contact cycles, even though FTIR spectra of AD-AR2 also exhibited pH dependent formation and dissociation of catechol-boronate complex. This further confirmed that the poor adhesive property of AD-AR2 is due to reduced coverage of the coated adhesive.

AD-Flat also demonstrated appreciable W_{adh} value during the first contact cycle at pH 3 ($W_{adh} = 262.3 \pm 17.67$ mJ/m^2) (Figure 6a). However, the W_{adh} value did not diminish significantly during the second contact cycle at pH 9 ($W_{adh} = 162.1 \pm 14.21$ mJ/m^2) and the adhesive did not recover during the third contact cycle at pH 3 ($W_{adh} = 196.9 \pm 66.40$ mJ/m^2) (Table S12). FTIR spectra indicated the presence of the catechol-boronate complex peak after the second contact cycle (pH 9), which continued to exist even after the third contact cycle (pH 3) (Figure S6). This indicated that a short 5 min incubation period in between contact cycles was insufficient to completely break the complex due to slow diffusion of ions into the bulk of AD-Flat. To break the complex, it is necessary to change the pH within the adhesive network to an acidic pH. This requires diffusion of sufficient amount of proton ions to enter the adhesive network from the surrounding medium. However, due to large gel volume, this diffusion process is slow. This is in agreement with our previous studies, which indicated that 30-60 min of incubation was required for reversible transitions between strong and weak adhesion for hydrogel-based adhesives.[15, 16] On the other hand, coating the adhesive onto micropillars greatly increased the surface area to volume ratio of the hydrogel network, which enhanced the rate diffusion of ions from the surrounding medium into the network. This results in a faster change of pH and increased rate of formation or dissociation of the complex. All unmodified, bare micropillars exhibited low adhesion values and were not responsive to pH changes (Figure S7).

To further investigate the adhesion switching capabilities of AD-AR1, the incubation time between cycles was decreased from 5 min to 1 min (Figure 7). AD-AR1 repeatedly exhibited elevated adhesive property ($W_{adh} = 450$-550 mJ/m^2 and $S_{adh} = 18$-22 kPa) when tested at pH 3 and significantly reduced adhesive property ($W_{adh} = 250$-300 mJ/m^2 and $S_{adh} \sim 5$ kPa) when tested at pH 9. There was no significant reduction in the measured adhesive strength over the 8 contact cycles. The FE-SEM image of AD-AR1 obtained at the end of these tests also indicated no observable structural damage (Figure S10). However, adhesion values obtained after 1 min of incubation at pH 9 were much higher when comparing to those obtained after 5 min incubation ($W_{adh} = 120$ mJ/m^2 and $S_{adh} \sim 1$ kPa, Figure 6). This indicates that there were still incomplete complex formation after only 1 min of incubation. This resulted in free catechol and phenylboronic acid moieties available for interfacial binding, which contributed to higher adhesive values when compared to 5 min incubation. An incubation time longer than 1 min may be needed to completely deactivate the adhesive.

Taken together, our results confirmed previous findings that the presence of catechol is required to impart PDMS-based pillars with elevated adhesion to wetted surfaces.[19–21] However, these previous findings utilized adhesive coatings that contained only catechol and cannot be inactivated. Recently, micropillar coated with catechol-modified poly(*N*-isopropylacrylamide)-based polymer demonstrated tunable adhesive property in response to changes in temperature.[40] However, in the absence of a protecting group, the binding

strength of catechol decreased with increasing incubation time in elevated temperature[40] and pH.[41] Unlike these previous reports, we incorporated network-bound phenylboronic acid that acted as a temporary protecting group for preventing catechol oxidation at a basic pH. Additionally, incorporation of phenylboroinc acid has been previously demonstrated to enhance adhesion to both inorganic Si surface and biological substrates, such as the mucosal lining of the gastrointestinal tract.[42] We previously reported that hydrogels containing phenylboronic acid alone demonstrated strong adhesion to quartz substrate under wetted conditions, with work of adhesion values that were equivalent to that of DMA-containing hydrogel.[15] However, the adhesive property of bonronic acid was not pH responsive and both catechol and boronic acid were essential in the design of a smart adhesive.[15]

Micropillars coated with an adhesive containing both DMA and AAPBA demonstrated multiple cycles of reversible and tunable interfacial binding property (Scheme 1). When compared to hydrogel-based adhesives that responded slowly to change in pH,[15, 16] adhesive-coated pillars reported here exhibited significantly faster rate of transition. This is because of the increased surface area to volume ratio of the pillar structures, which enhanced the diffusion of ions from the pH buffer into the adhesive. Thus, the change in pH within the adhesive was considerably quicker, which potentially led to faster formation and breaking of the catechol-boronate complex and consequent rapid adhesion switching. Additionally, the hydrogel coatings also contain significantly reduced volume needed for the pH to change within the adhesive network. Although the current study focused on tuning the adhesive property of catechol-based smart adhesive at pH 3 and 9, it is potentially feasible to tune the complexation pH by incorporating anionic species into the adhesive coating so that it could demonstrate strong adhesion at physiological and marine pH ranges.[16] For uncoated pillared structures, dry adhesion typically increases with increasing AR.[26] However, for the hydrogel-coated pillars reported here, pillars with AR of 2 did not exhibit adhesion to wetted surfaces. This is potentially due to insufficient coverage of the micropillars with the adhesive coating due to significantly higher interstitial volume. Alternative coating methods are potentially needed to enable these pillars with wet adhesive property.

Conclusions

PDMS micropillars were coated with adhesive hydrogel containing network-bound dopamine and phenylboronic acid. The presence of the adhesive coating was verified using FE-SEM, FTIR, XPS, and contact angle measurements. These adhesive-coated pillars exhibited reversible and tunable adhesive property in response to changing pH. The rate of change was significantly higher when compared to bulk adhesive hydrogel with the same composition. The elevated surface area to volume ratio of the micropillars increased the rate of ion diffusion and contributed to the increased rate of formation and breaking of catechol-boronate complex.

Supplementary Material

Refer to Web version on PubMed Central for supplementary material.

Acknowledgements

References

1. Pinnaratip R, Bhuiyan MSA, Meyers K, Rajachar RM and Lee BP, Advanced Healthcare Materials, 2019, 1801568.

2. Heinzmann C, Coulibaly S, Roulin A, Fiore GL and Weder C, ACS Appl. Mater. Interfaces, 2014, 6, 4713–4719. [PubMed: 24484360]

3. Luo X, Lauber KE and Mather PT, Polymer, 2010, 51, 1169–1175.

4. Banea MD, da Silva LFM, Carbas RJC and de Barros S, The Journal of Adhesion, 2017, 93, 756–770.

5. Gao Y, Wu K and Suo Z, Adv Mater, 2019, 31, e1806948. [PubMed: 30549118]

6. Northen MT, Greiner C, Arzt E and Turner KL, Adv. Mat, 2008, 20, 3905–3909.

7. Lee BP, Messersmith PB, Israelachvili JN and Waite JH, Annu. Rev. Mater. Res, 2011, 41, 99–132. [PubMed: 22058660]

8. Lu Q, Danner E, Waite JH, Israelachvili JN, Zeng H and Hwang DS, Journal, 2013, 10, 20120759.

9. Liu Y, Meng H, Konst S, Sarmiento R, Rajachar R and Lee BP, ACS Appl. Mater. Interfaces, 2014, 6, 16982–16992. [PubMed: 25222290]

10. Meredith HJ and Wilker JJ, Advanced Functional Materials, 2015, 25, 5057–5065.

11. Pechey A, Elwood CN, Wignall GR, Dalsin JL, Lee BP, Vanjecek M, Welch I, Ko R, Razvi H and Cadieux PA, J Urol, 2009, 182, 1628–1636. [PubMed: 19683735]

12. Shafiq Z, Cui J, Pastor-Pérez L, San Miguel V, Gropeanu RA, Serrano C and del Campo A, Angew. Chem., Int. Ed, 2012, 51, 4332–4335.

13. Wilke P, Helfricht N, Mark A, Papastavrou G, Faivre D and Börner HG, J. Am. Chem. Soc, 2014, 136, 12667–12674. [PubMed: 25133879]

14. Ma Y, Ma S, Wu Y, Pei X, Gorb SN, Wang Z, Liu W and Zhou F, Advanced Materials, 2018, 1801595.

15. Narkar AR, Barker B, Clisch M, Jiang J and Lee BP, Chemistry of Materials, 2016, 28, 5432–5439. [PubMed: 27551163]

16. Narkar AR and Lee BP, Langmuir, 2018, 34, 9410–9417. [PubMed: 30032614]

17. Spolenak R, Gorb S and Arzt E, Acta Biomaterialia, 2005, 1, 5–13. [PubMed: 16701776]

18. Huber G, Mantz H, Spolenak R, Mecke K, Jacobs K, Gorb SN and Arzt E, Proceedings of the National Academy of Sciences of the United States of America, 2005, 102, 16293–16296. [PubMed: 16260737]

19. Lee H, Lee BP and Messersmith PB, Nature, 2007, 448, 338–341. [PubMed: 17637666]

20. Glass P, Chung H, Washburn NR and Sitti M, Langmuir, 2009, 25, 6607–6612. [PubMed: 19456091]

21. Glass P, Chung H, Washburn NR and Sitti M, Langmuir, 2010, 26, 17357–17362. [PubMed: 20879746]

22. Zhang H, Bian C, Jackson JK, Khademolhosseini F, Burt HM and Chiao M, ACS Applied Materials & Interfaces, 2014, 6, 9126–9133. [PubMed: 24853631]

23. Lee BP and Konst S, Advanced Materials, 2014, 26, 3415–3419. [PubMed: 24596273]

24. Lee BP, Lin M-H, Narkar A, Konst S and Wilharm R, Sens. Actuators, B, 2015, 206, 456–462.

25. Cuchiara MP, Allen AC, Chen TM, Miller JS and West JL, Biomaterials, 2010, 31, 5491–5497. [PubMed: 20447685]

26. Greiner C, del Campo A and Arzt E, Langmuir, 2007, 23, 3495–3502. [PubMed: 17315904]

27. Hertz H, J. Reine Angew Math., 1881, 92, 156–171.

28. Shull KR and Chen W-L, Interface Science, 2000, 8, 95–110.

29. Burkett JR, Wojtas JL, Cloud JL and Wilker JJ, The Journal of Adhesion, 2009, 85, 601–615.

30. Sharma D, Jia W, Long F, Pati S, Chen Q, Qyang Y, Lee B, Choi CK and Zhao F, Bioactive Materials, 2019, 4, 142–150. [PubMed: 30873506]

31. Wang P, Su J, Shen M, Ruths M and Sun H, Langmuir, 2017, 33, 638–644. [PubMed: 27973850]

32. Johnson LM, Gao L, Shields IV CW, Smith M, Efimenko K, Cushing K, Genzer J and López GP, Journal of nanobiotechnology, 2013, 11, 22. [PubMed: 23809852]

33. Park JK, Kim KS, Yeom J, Jung HS and Hahn SK, Macromol. Chem. Phys, 2012, 213, 2130–2135.

34. Faniran J and Shurvell H, Canadian Journal of Chemistry, 1968, 46, 2089–2095.

35. Parkinson C, Walker M and McConville C, Surface Science, 2003, 545, 19–33.

36. Podsiadlo P, Kaushik AK, Arruda EM, Waas AM, Shim BS, Xu J, Nandivada H, Pumplin BG, Lahann J and Ramamoorthy A, Science, 2007, 318, 80–83. [PubMed: 17916728]

37. Feng B, Zhang J, Zhong Q, Li W, Li S, Li H, Cheng P, Meng S, Chen L and Wu K, Nature chemistry, 2016, 8, 563.

38. Autumn K, Sitti M, Liang YA, Peattie AM, Hansen WR, Sponberg S, Kenny TW, Fearing R, Israelachvili JN and Full RJ, Proceedings Of The National Academy Of Sciences Of The United States Of America, 2002, 99, 12252–12256. [PubMed: 12198184]

39. Chen GC, Wood and Fiber science, 2008, 40, 248–257.

40. Zhao Y, Wu Y, Wang L, Zhang M, Chen X, Liu M, Fan J, Liu J, Zhou F and Wang Z, Nat Commun, 2017, 8, 2218. [PubMed: 29263405]

41. Zhong C, Gurry T, Cheng AA, Downey J, Deng Z, Stultz CM and Lu TK, Nat Nanotechnol, 2014, 9, 858–866. [PubMed: 25240674]

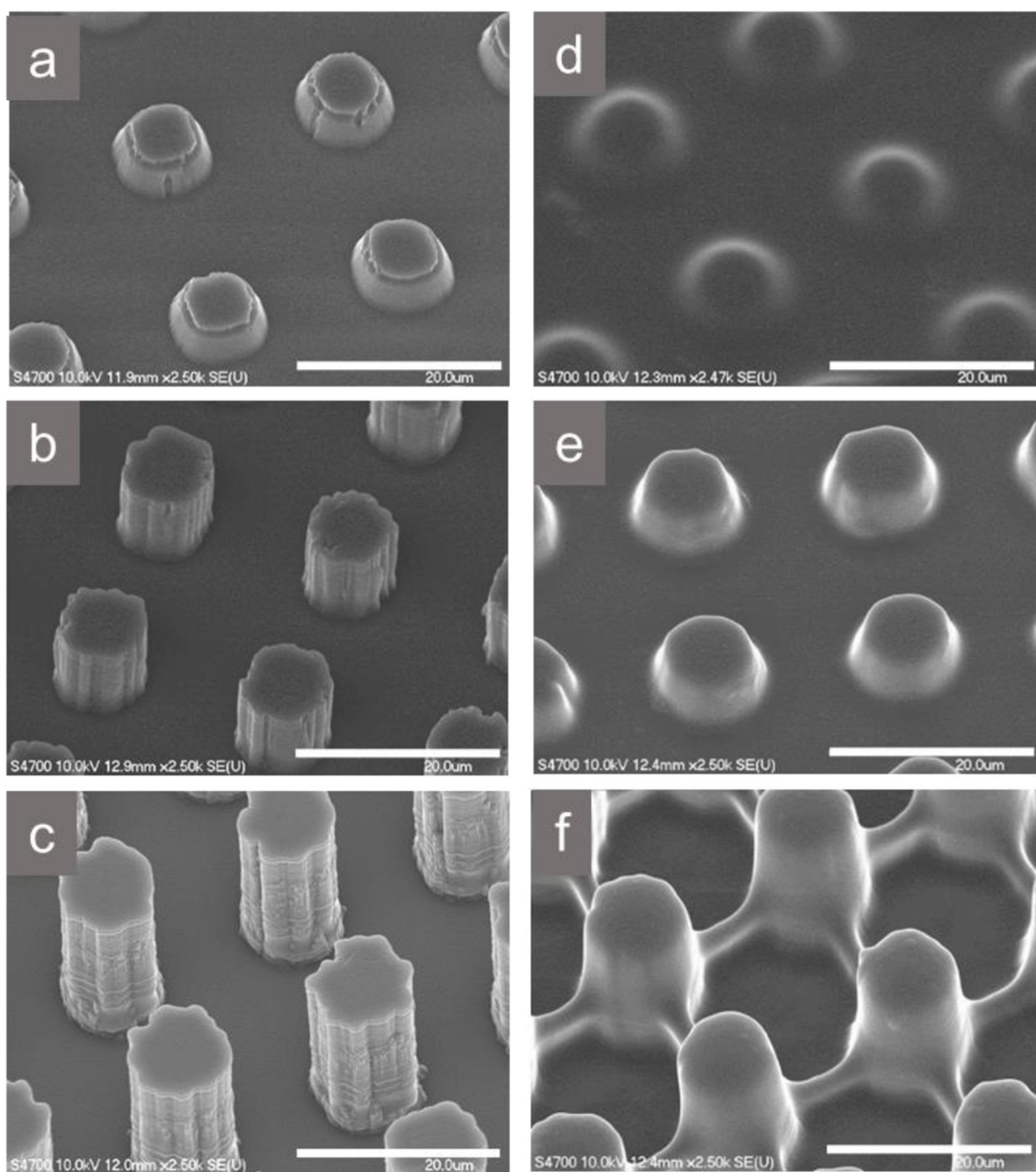42. Hong SH, Kim S, Park JP, Shin M, Kim K, Ryu JH and Lee H, Biomacromol., 2018, 19, 2053–2061.

Figure 1.
FE-SEM images of bare (Bare-AR0.4 (a), Bare-AR1 (b), and Bare-AR2 (c)) and adhesive hydrogel-coated (AD-AR0.4 (d), AD-AR1 (e), and AD-AR2 (f)) micropillars. Scale bar = 20 μm.
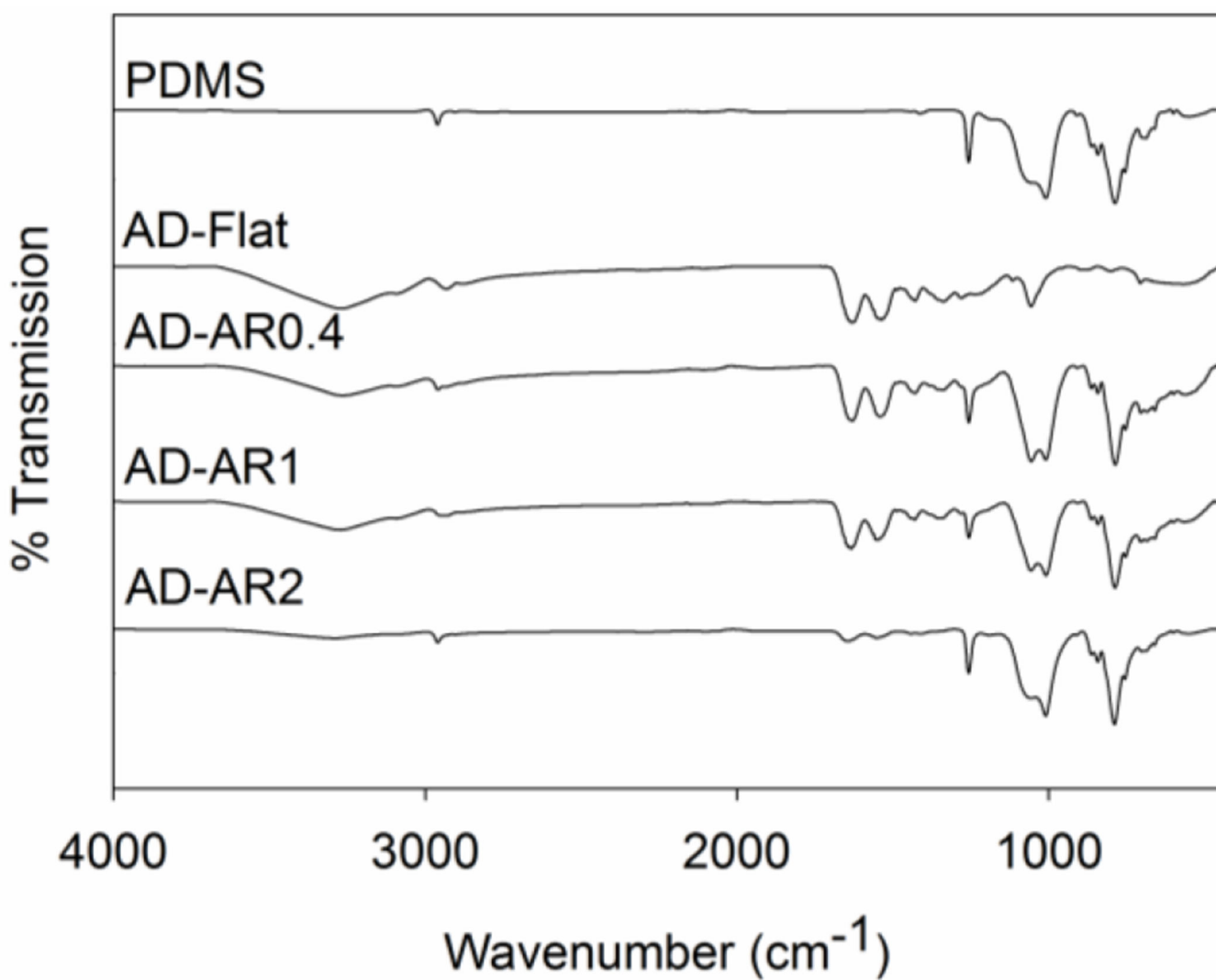
Figure 2.
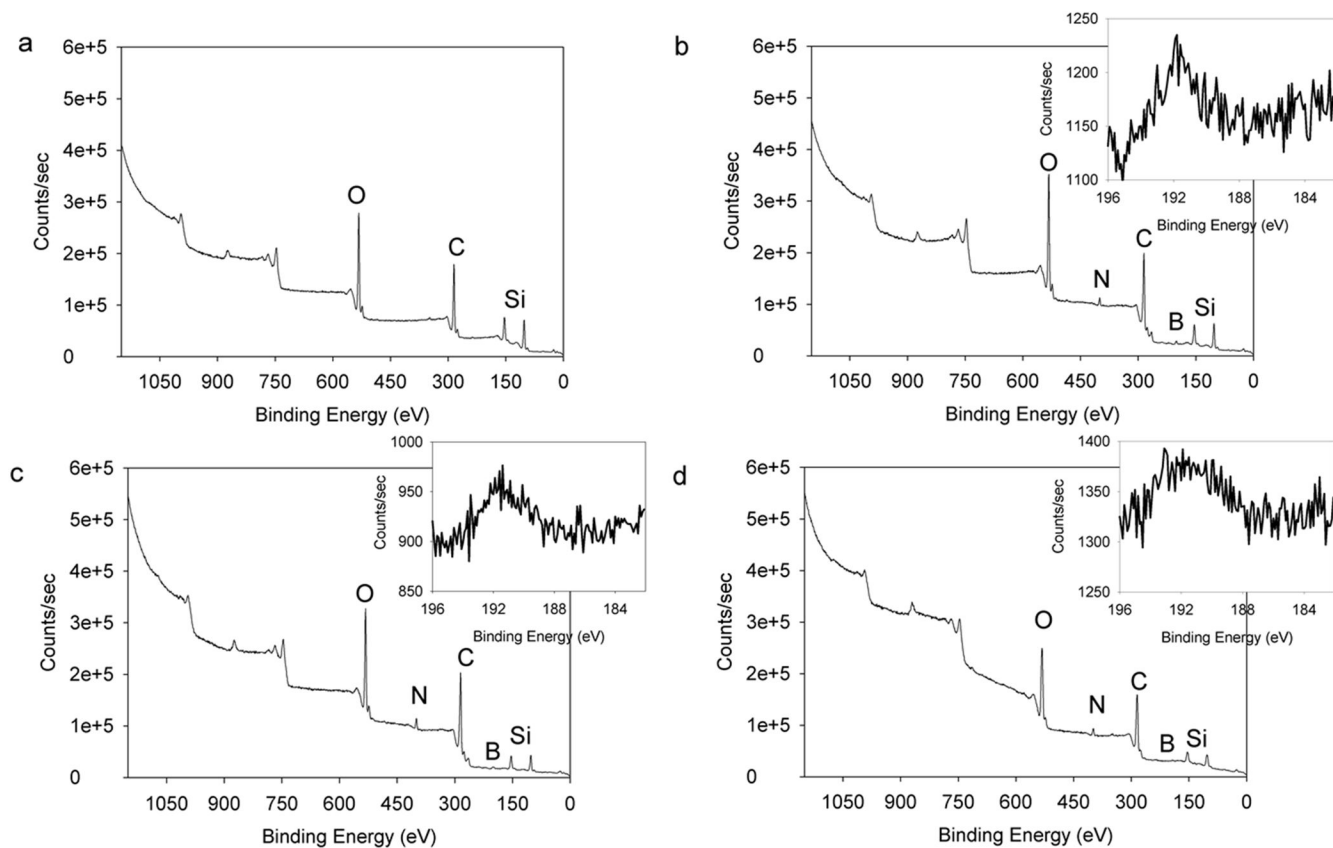FTIR spectra of unmodified PDMS, AD-Flat, AD-AR0.4, AD-AR1, AD-AR2 tested at pH 3.

Figure 3.
XPS spectra of Bare-AR1 (a), AD-AR0.4 (b), AD-AR1 (c), and AD-AR2 (d). The inset images in b, c, and d show the presence of boron 1s orbital with binding energy of 191.5 eV.
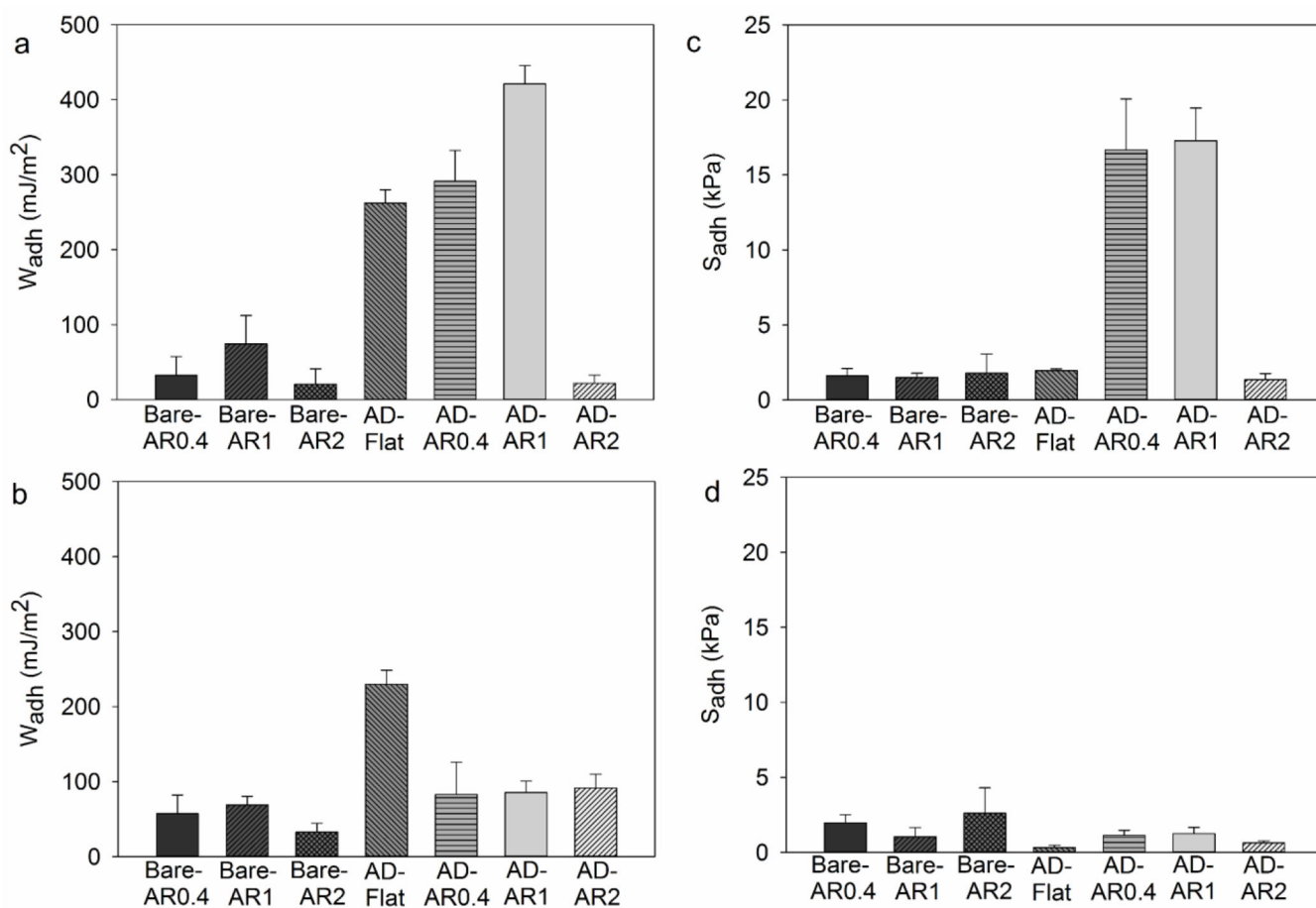
Figure 4.
W_{adh} (a, b) and S_{adh} (c, d) for adhesive tested at pH 3 (a, c) and 9 (b, d) (n = 3). Refer to Tables S1 and S2 for statistical analysis.
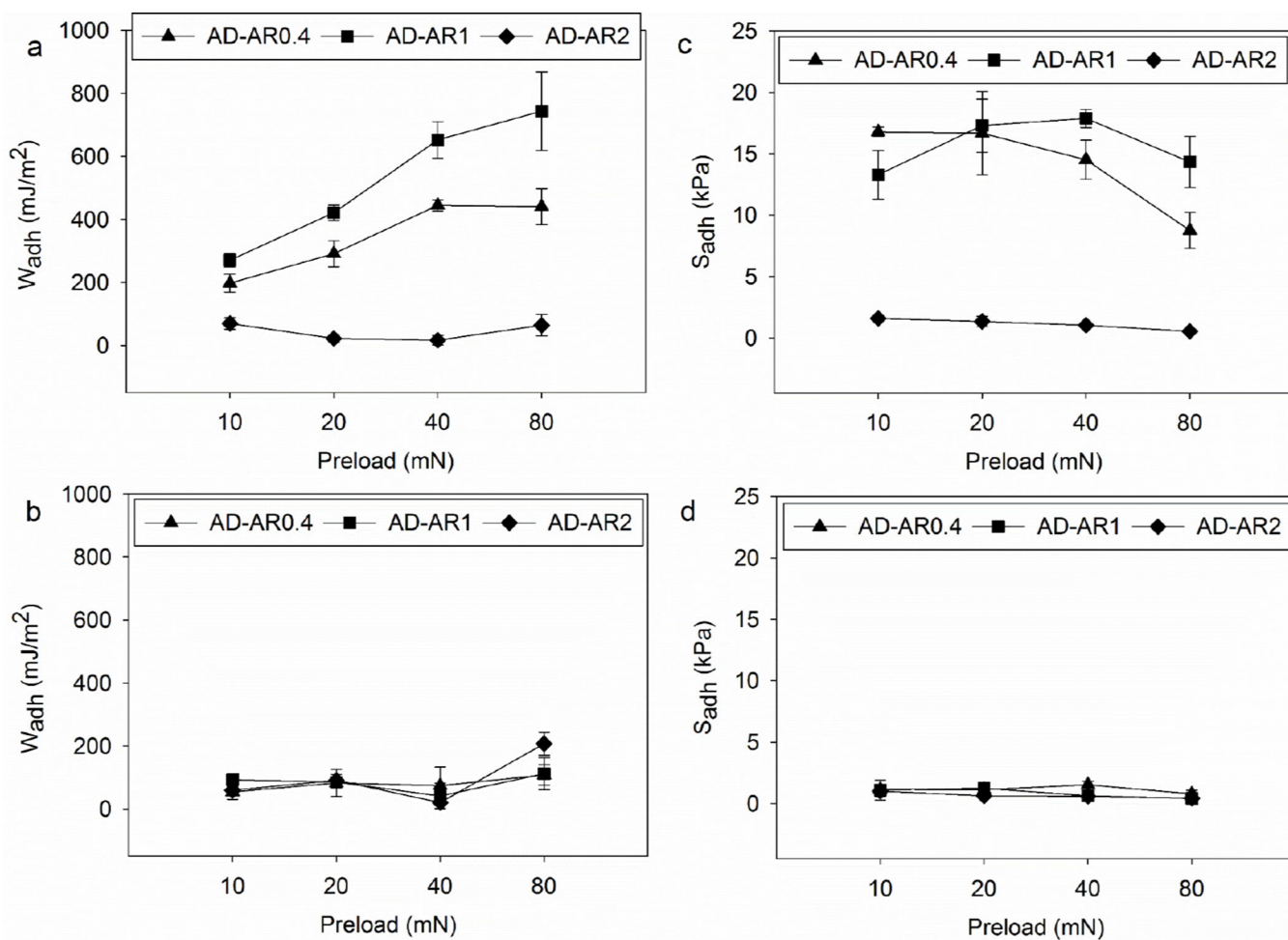
Figure 5.
W_{adh} (a, b) and S_{adh} (c, d) for adhesive tested at pH 3 (a, c) and 9 (b, d) tested at varying preload (10-80 mN) (n = 3). Refer to Tables S3–S6 for statistical analysis.
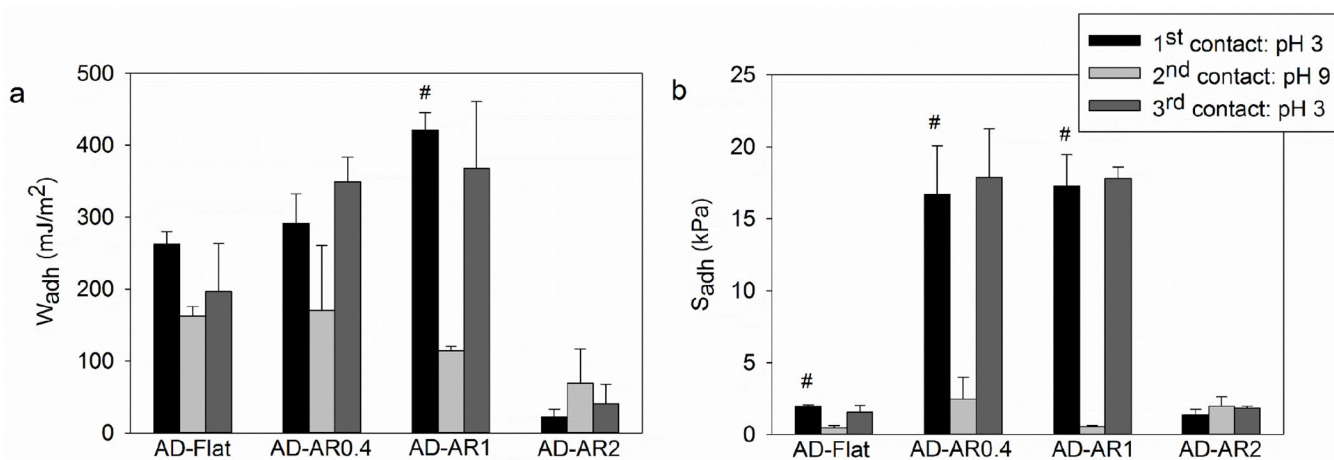
Figure 6.
Work of adhesion (W_{adh}) (a) and strength of adhesion (S_{adh}) (b) for AD-Flat and adhesive hydrogel-coated micropillars with different ARs tested in 3 successive contact cycles with 5 min incubation time in between cycles (n = 3). # $p < 0.05$ when compared to the value of the 2nd contact cycle for a given composition. Refer to Tables S12–S15 for further statistical analysis.
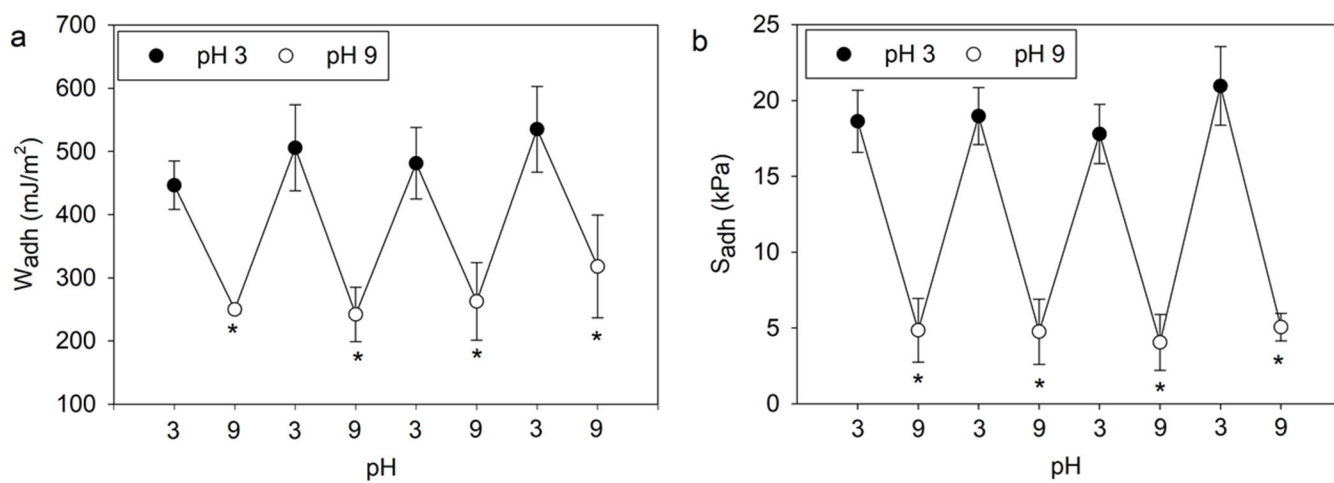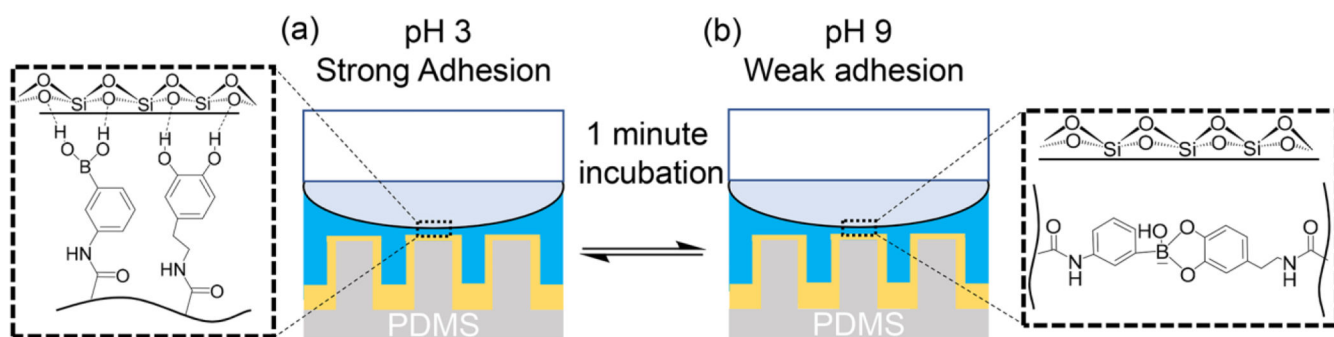
Figure 7.
W_{adh} (a) and S_{adh} (b) for AD-AR1 tested in successive contact cycles with 1 min incubation time in between cycles (n = 3). * $p < 0.05$ when compared to the preceding contact cycle at pH 3.

Author Manuscript Author Manuscript Author Manuscript Author Manuscript

Scheme 1.
Rapid adhesion switching of smart adhesive-coated pillars showing strong adhesion at pH 3 (a) and weak adhesion at pH 9 (b) with just 1 minute incubation between contact cycles.

Table 1.

Average water contact angles for bare and adhesive hydrogel-coated micropillars with differen aspect ratios (n = 3).

Aspect ratio (AR)	Contact angle in degree (°)	
	Bare micropillars (Bare-ARx)	Adhesive hydrogel-coated micropillars (AD-ARx)
0.4	135.6 ± 0.80	113.3 ± 6.1
1	146.9 ± 1.7	115.3 ± 1.9
2	149.4 ± 0.60	129.2 ± 1.5